PERGAMON

Journal of Structural Geology 24 (2002) 1013–1028

JOURNAL OF STRUCTURAL GEOLOGY

www.elsevier.com/locate/jstrugeo

Microprobe monazite geochronology: putting absolute time into microstructural analysis

Michael L. Williams*, Michael J. Jercinovic

Department of Geosciences, Morrill Science Center, University of Massachusetts, 611 North Pleasant St., Amherst, MA 01003-9297, USA

Received 21 February 2001; revised 15 June 2001; accepted 15 June 2001

Abstract

High-resolution compositional mapping and dating of monazite on the electron microprobe is a powerful addition to microstructural analysis and an increasingly important tool for tectonic analysis. Microprobe monazite geochronology can be an efficient reconnaissance tool for evaluating metamorphic and deformational age domains, but more importantly, its in-situ nature and high spatial resolution offer an entirely new level of structurally and texturally specific geochronologic data that can be used to put absolute time constraints on *P–T–D* paths, constrain the rates of metamorphic and deformational processes, and provide new links between metamorphism and deformation. Microprobe geochronology is particularly applicable to three persistent microstructural/microtextural problem areas: (1) constraining the chronology of metamorphic assemblages; (2) constraining the timing of deformational fabrics; and (3) interpreting other geochronological results. Although some monazite generations can be directly tied to metamorphism or deformation, at present, the most common constraints rely on monazite inclusion relations in porphyroblasts that, in turn, can be tied to the deformation and/or metamorphic history. Microprobe mapping and dating allow geochronology to be incorporated into the routine microstructural analytical process, resulting in a new level of integration of time (*t*) into *P–T–D* histories.

Keywords: Compositional mapping; Microprobe monazite geochronology; Microstructural analysis; Tectonic analysis

1. Introduction

Most tectonites contain evidence for more than one ‘deformation event’. Multiple fabrics, contrasting shear sense indicators, or evidence of deformation under distinctly different conditions all suggest that rocks preserve evidence of earlier stages in their structural evolution. Similarly, relict metamorphic minerals or disequilibrium assemblages are indications of earlier *P–T* conditions in a tectonic history. One of the most fundamental questions in microstructural analysis concerns whether multiple tectonic fabrics represent stages in a single tectonic cycle or distinct tectonic events. For example, evidence for three or more *P–T–D* (pressure–temperature–deformation) loops exists in some Proterozoic rocks of the southwestern USA (Fig. 1), but it is unclear if these represent local thermal spikes associated with plutonism or separate collisional orogenic events (Bishop, 1997). Because of this uncertainty, the degree to which the *P–T–D* loops can or should be correlated across larger parts of an orogenic belt is also unclear. Yet, the correlation of deformation and metamorphic events is critical for building tectonic models.

Although *P–T–D* paths in themselves can provide great insight into tectonic processes, absolute time (*t*), is essential for interpreting the full tectonic significance of fabrics and textures and for developing an understanding of the evolution and rates of tectonic processes in multiply deformed metamorphic rocks. Great progress has been made in refining geochronologic techniques, particularly for metamorphic tectonites. U–Pb isotope dates are commonly obtained from single crystals of zircon, monazite, or titanite with precision on the order of one million years, and multiple isotopic systems can be combined to yield more than one point in a *P–T–D* history. However, the presence of multiple fabrics, assemblages, or *P–T–D* loops can lead to ambiguities about which part of the *P–T–D* history has actually been dated. In addition, even single crystals of monazite or zircon can have more than one age domain, reflecting different stages in the geologic history (Zhu et al., 1997; Williams et al., 1999a; Schmitz and Bowring, 2000). For tectonic studies of polygenetic rocks, it is essential to have in-situ age constraints in order to link specific dates to specific structural or textural domains.

* Corresponding author. Tel.: +1-413-545-0745; fax: +1-413-545-1200.
E-mail address: mlw@geo.umass.edu (M.L. Williams).

0191-8141/02/$ - see front matter
PII: S0191-8141(01)00088-8

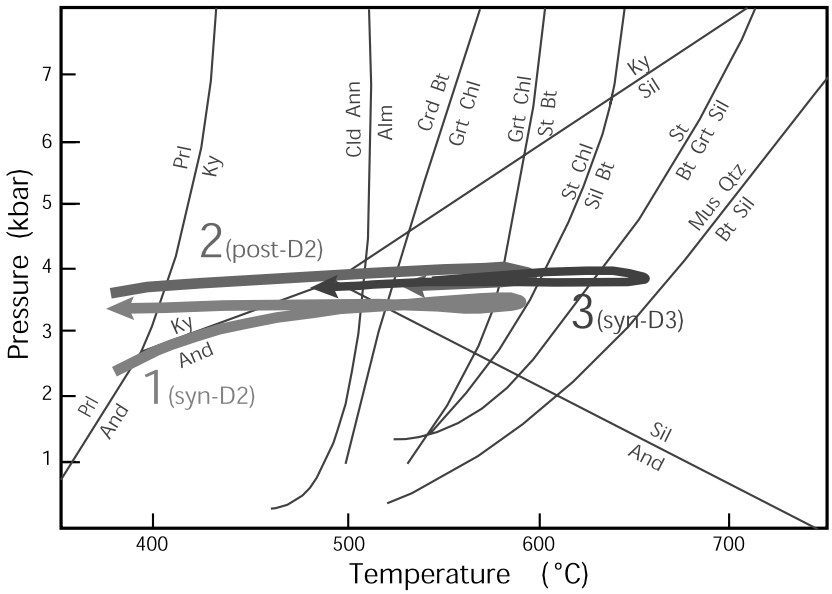

Fig. 1. Pressure–temperature (*P–T–D*) history for Proterozoic rocks of the Cerro Colorado area, Tusas Mountain New Mexico (after Bishop, 1997). Loops are based on porphyroblast–matrix inclusion relationships and on metamorphic equilibria and thermobarometry. D1, D2, and D3 correspond to deformation phases associated with the three main foliations (S1, S2, and S3) observed in the field and in thin section. Mineral abbreviations are after Kretz (1983). A persistent question concerns the absolute age and regional significance of the three loops. See text for discussion.

Electron microprobe 'chemical' dating of monazite offers a rapid, accurate, in-situ means of geochronology that is becoming a critical companion to other geochronologic techniques for tectonic analysis of metamorphic rocks. Because of its high spatial resolution, this technique provides an unprecedented level of geochronologic detail that can be used to unravel complex tectonic histories and aid in the interpretation of companion geochronologic data (Montel et al., 1996, 2000; Cocherie et al., 1998; Williams et al., 1999a). The purpose of this paper is to illustrate the application of electron microprobe dating to three specific microstructural/microtextural problems: (1) constraining the timing of metamorphic assemblages; (2) constraining the timing of deformational fabrics; and (3) interpreting complex geochronologic data sets. In each case, monazite compositional mapping and dating by electron microprobe offer new insights into the tectonic history of the region of interest, and into microstructural processes in general. Microprobe mapping and dating allow geochronology to be incorporated into the microstructural analytical process, resulting in a new level of integration of time (*t*) into *P–T–D* histories.

Perhaps the major conclusion of this work is that monazite geochronology is most powerful when combined with detailed, process-oriented microstructural analysis. Such analyses have been taught and carried out by Ron Vernon for thirty years. The onset of microprobe monazite geochronology adds new incentive and new power to microstructural analysis, and thus will further increase the need for the tools that Ron has helped to develop.

2. Background

Monazite is a rare-earth-element phosphate mineral, (Ce, La, Nd, Th, Y)PO_4, that is present as an accessory phase in many igneous and metamorphic rocks. Because it contains significant amounts of Th and U, with little common Pb, it has been widely used for U–Pb dating (Parrish, 1990). Also, because diffusion of major and trace components is extremely slow (cf. Parrish, 1990; Cherniak et al., 2000), monazite has the potential to retain chemical and geochronological information through younger metamorphic events.

Recent work has demonstrated that electron microprobe analysis can be a precise method for dating monazite (e.g. Suzuki and Adachi, 1991, 1998; Suzuki et al., 1994; Montel et al., 1996, 2000; Cocherie et al., 1998; Williams et al., 1999a; Hanchar et al., 2000; Jercinovic and Williams, 2000; Livi et al., 2000; Terry et al., 2000; Williams and Jercinovic 2000a,b; Shaw et al., 2001). The age is determined by measuring the concentration of U, Th, and Pb, with the assumptions that there is negligible common lead, that the isotopes of U are present in their crustal abundances, and that elemental concentrations have not been significantly modified by subsequent mass transfer (Montel et al., 1996; Cocherie et al., 1998). Much of the existing work has been carried out on monazite crystals separated from the host rock and prepared for microanalysis as grain mounts. Dating these materials has revealed multiple stages of crystal growth and complex histories for monazite which have, in some cases, clarified the interpretation of dates previously obtained by conventional mass spectrometry (e.g. Cocherie

et al., 1998; Bosbyshell and Jercinovic, 1999; Crowley and Ghent, 1999). Backscattered electron images have been used to identify compositional domains in individual monazite grains (Montel et al., 1996; Cocherie et al., 1998). However, BSE contrast tends to reflect Th variation and may not necessarily relate directly to age domains. Williams et al. (1999a) used high-resolution wavelength dispersive compositional maps to characterize compositional and age domains in individual monazite crystals, and found that careful analyses within compositional domains can yield accurate dates with precision on the order of 5–10 my.

2.1. Geologic background

The examples cited below come from two general areas, each nearly ideally suited to the application of microprobe geochronology. Most come from the Proterozoic orogenic belt of the southwestern USA. There, Paleoproterozoic sedimentary and volcanic rocks were deformed and metamorphosed in a series of events that reflect a long-lived accretionary continental margin, active from ca. 1800 to 1000 Ma (Karlstrom et al., 2001). In Arizona, northern New Mexico, and southern Colorado, the Proterozoic rocks were deformed and metamorphosed during at least two major events, the 1750–1650 Ma Yavapai/Mazatzal orogeny and a second progressive event (ca. 1450–1350 Ma) that corresponds to a period of widespread granite plutonism (Anderson, 1989). The rocks are interpreted to have been buried to mid-crustal levels during the early parts of the first event, and most of the region remained at mid-crustal levels until after the second event and locally much longer (Williams and Karlstrom, 1996; Karlstrom and Williams, 1998; Williams et al., 1999b).

Peak metamorphic temperatures varied in relation to syntectonic plutons during both tectonic events (Nyman et al., 1994; Karlstrom and Williams, 1995). Thus, because of the similar pressures, similar metamorphic grades and gradients have been superimposed (Fig. 1). Traditionally, most of the structures, fabrics, and regional metamorphic assemblages, including widespread Al-silicate triple point metamorphism, have been attributed to the Yavapai/Mazatzal event (1720–1650 Ma), but in several areas, intense deformation and metamorphism have recently been constrained to the younger (ca. 1400 Ma) event (Grambling and Dallmeyer, 1993; Daniel et al., 1995; Bishop, 1997; Wingsted, 1997; Williams et al., 1999b). In order to understand the accretion, evolution, and ultimate stabilization of the southern margin of Laurentia, it is critical to distinguish and characterize the various stages in the long tectonic history, but due to the overprinting of similar grades and styles, this has proven to be difficult.

Several additional examples come from northernmost Saskatchewan in the western Canadian Shield. There, granulite facies mylonites were developed in a series of tectonic events from at least 2600 Ma to 1800 Ma. The most striking feature in the area is the Striding–Athabasca mylonite zone, a portion of the Snowbird tectonic zone that separates the Rae and Hearne Archean crustal provinces (Hanmer, 1997). The Striding–Athabasca mylonite zone underwent granulite facies mylonitic deformation at 2600 Ma, apparently in the deep crustal (ca. 1.0 GPa) parts of a transcurrent, intracontinental shear zone. After this event, or series of events, the rocks apparently remained in the deep crust, and were periodically reactivated until at least 1900 Ma. Between 1900 and 1800 Ma, rocks of the Striding–Athabasca mylonite zone were locally overprinted by granulite facies assemblages and fabrics, and rocks to the west were penetratively deformed and metamorphosed (Williams et al., 2000). This event culminated in exhumation, but the detailed timing is poorly constrained. The rocks provide a special opportunity to investigate deep crustal processes and the exhumation of regional granulite terrains, but it is essential to distinguish fabrics and textures that formed in the deepest crust from those that developed later during the exhumation process.

3. Methods

Monazite microprobe analyses have been carried out on a four-spectrometer Cameca SX50 electron microprobe, employing Cameca's automation and data reduction software. Matrix corrections were done using the PAP method (Pouchou and Pichoir, 1984, 1985). The basic procedure for monazite identification, compositional mapping, and analysis is outlined in Table 1. Several aspects of the procedure will be highlighted here because of their direct relevance to microstructural analysis.

3.1. Monazite identification and microstructural classification

Perhaps the most critical step in microstructurally-relevant monazite geochronology is to identify all monazite grains in a thin section so that populations can be correlated with particular structural or metamorphic settings. Full-section monazite location maps, generated by superimposing an enhanced Ce image over a simultaneously collected reference image (typically Al, Ca, or Mg) provide an efficient means of placing monazite grains into their geologic context. For example, Fig. 2 shows a full-section map of a thin section from the Upper Granite Gorge of the Grand Canyon. The section has three major microstructural domains, a large garnet porphyroblast, leucosome tails, and matrix. Each of the domains contain monazite allowing constraints to be placed on the age of garnet growth, partial melting, and final matrix recrystallization, respectively (see below). This search method has the benefit of locating all monazite crystals in the mapped area, including a significant population less than 10 μ in size, a population not typically sampled by other techniques.

Table 1
Procedures for microstructural analysis, compositional mapping, and dating of monazite on the electron microprobe

Step	Procedure	Explanation
1	Generate full section map	Collect maps of Ce to identify monazite occurrences, along with a reference element (usually Mg or Al) to record texture: Stage scan mapping, 1024 × 512 pixels, 35 micron steps, beam defocussed (35 microns), 350 nA, 10 ms count time/pixel (Fig. 1).
2	Process maps and identify 'critical' monazite	Adjust input and output levels in Ce maps to bring out low level Ce counts, mark Ce spots on new image layer and overlay this layer on top of reference map. Identify monazite grains to analyze by referring to their relation to microstructure, host minerals, etc.
3	Map individual monazite grains	Map selected monazite grains (from step 2, above) at high magnification: Beam scanning, 200 nA, focussed beam; step sizes <1 μm. Map for Y, Th, Pb, U.
4	Generate 'age' maps	Calculate approximate Th, Pb, U concentrations for individual pixels in high-resolution monazite maps: Estimate k-ratios by subtracting backgrounds and referencing pixel counts to standard intensities; apply 'typical' PAP factors to resultant ratios to obtain approximate concentrations. Then, calculate (by iteration of the age equation), relative age values for each pixel, and reassemble into complete 'age' map.
5	Obtain major element analyses	Quantitatively analyse the selected monazite for major element concentrations. Generally P, Ca, Y, Th, U, As and the light rare-earths.
6	Obtain trace element analyses	Enter representative major element analysis into the trace program, then calibrate and analyze the selected monazite grains for Y, Th, Pb, U. Domains in individual grains can be identified based on inspection of age maps and compositional maps.
7	Calculate dates	Dates for individual points are calculated iteratively by entering an age estimate into the age equation with the known concentrations of Th and U, and calculating the expected Pb concentration. The date is varied until the calculated Pb matches the measured Pb.
8	Document and evaluate final point locations	Capture high magnification backscatter images of analyzed grains to precisely locate trace element analysis points. This image is then used to generate an outline, with points marked, which is scaled and overlayed onto monazite compositional maps. Points compromised by overlap of domain boundaries are easily identified and excluded.

3.2. Monazite compositional mapping and age mapping

Monazite crystals, once identified and classified according to microstructural and metamorphic setting, are mapped at high resolution for Y, Th, U, and Pb. These maps reveal, in nearly all monazite, considerable compositional heterogeneity that can commonly be related to microstructure or texture (see Table 2). Significantly, domain boundaries are typically sharp indicating little modification by diffusion. Age maps are constructed from individual element maps by calculating a U–Th–Pb date for each pixel (Williams et al., 1999a). For example, a monazite crystal from the Homestake shear zone, Colorado has an obvious Th-, Y- and Pb-rich core domain and distinct overgrowth 'tips' (Fig. 3). However, the age map shows that one tip is only slightly younger than the core whereas the other is

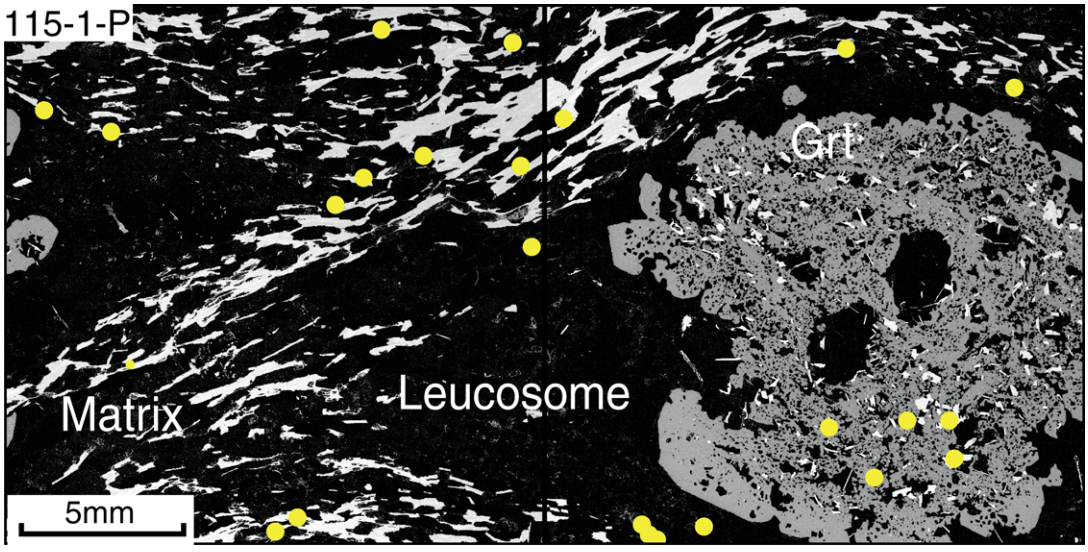

Fig. 2. Full thin section image showing location of monazite. The thin section is from a migmatite from mile 115 in the Upper Granite Gorge of the Grand Canyon. Garnet (large gray porphyroblast at right) is associated with leucosome tails (dark) in a biotite–quartz–plagioclase matrix. The image was constructed by superimposing a $Ce_{L\alpha}$ image (yellow dots) on $Mg_{K\alpha}$ (reference element). Note that monazite occurs as inclusions in garnet, in leucosome, and in the matrix.

Table 2
Monazite compositions and geochronologic data

Sample	Figure	Domain	Trace element analyses (in ppm)					Date[a]	Std Err[b]
			Y	Th	Pb[c]	U	*N*	(Ma)	(Ma)
HS12-M3	3, 4	Core	23,650	68,660	7064	6437	9	1661	3.3
	3, 4	Over-1	23,618	58,862	6360	6992	5	1638	7.3
	3, 4	Over-2	13,664	60,294	4852	4479	3	1398	8.5
99W19bM20	5	Core	12,148	12,386	1816	1876	14	2010	14.5
	5	Rim	5,734	52,426	5891	3948	9	1888	5.5
99W19bM15	5	Core	9,605	29,647	2979	1044	8	1910	10.1
	5	Median	3,800	51,518	5114	2177	12	1848	6.0
	5	Rim	69	51,983	5045	2260	15	1803	3.6
115PM3	6a,b	Core	11,060	12,500	2570	5240	3	1755	
	6a,b	Rim	4,945	16,890	1816	1885	5	1702	9.3
	6c	Core	7,909	11,629	2148	4435	5	1674	10.9
CC54b	7	All	3,981	24,759	2351	3370	13	1398	5.8
HS18M7	8	All	8,410	30,281	2335	1734	11	1387	6.7
M201	9	Low-Th Core	2,758	33,863	4424	1092	7	2450	4.5
	9	Rim	642	65,153	6348	2819	4	1809	6.7
CC56M8	10	All	10,117	43,914	3784	4148	4	1399	8.2
CC56M9	10	Core	13,938	23,377	3682	6608	1	1669	
	10	Rim	8,645	18,620	2082	3370	1	1468	
LGG245-3M2	11	Core	15,676	40,138	6376	6348	4	1688	1.2
	11	Rim	16,790	44,722	4573	4105	7	1659	6.6

[a] Dates are averages of '*N*' analyses carrried out in the same compositional domain.
[b] Std Err = One standard error of the mean. All analyses were done at: 200 nA, 15 kV, and 600 s.
[c] Pb measured on Pb Ma and corrected for YLγ interference. Detecton limits for trace element analyses are on the order of: Y: 20, Th: 40, Pb: 35, and U: 40 ppm.

approximately 250 my younger (see below for discussion). The relative magnitudes of the differences in age can be estimated using an image processor, before actually carrying out the quantitative analyses, by simply averaging pixel values within domains on the age map.

3.3. Quantitative monazite dating

Detailed spot analyses are then done to obtain precise dates for identified domains (Fig. 4). Several analyses, 5–10 spots if possible, are averaged within each compositional or age domain. Because it is critical to include only analyses that are entirely within domains, backscattered electron images, taken after analyses are completed, are generally superimposed onto the original compositional maps in order to identify 'successful' analyses (Fig. 4). These are averaged and standard errors of the mean are calculated. The statistics can be used to ask questions concerning the confidence with which the domains can be said to be distinct in age (Fig. 4b). We have tested the technique using a number of samples for which ages have been previously determined by conventional isotopic techniques (Williams et al., 1999a). In our work, we have found microprobe results to be in agreement with isotopic ages over a range from about 2600 to 270 Ma (see also Montel et al., 1996).

3.4. Evaluation of uncertainty

The quantification of uncertainty in microprobe monazite dating is a matter of current study. At present, reported dates and uncertainties are evaluated in the context of compositional and particularly, age maps. Age domains as determined from high-resolution mapping are taken to represent 'homogeneous' populations that are sampled during quantitative analysis. Unlike typical major-element silicate analyses, where single analyses are taken to characterize the composition at a point, we use the mean of a set of analyses (samples) as a basis for calculating a single date for a monazite domain. As discussed below, the precision is estimated for the domain, not for the individual analyses. Estimated ages and uncertainties can then be compared from domain to domain and from monazite grain to monazite grain in order to interpret the history of monazite growth events recorded in a particular rock or region.

The analytical precision associated with a microprobe date is primarily a function of Pb counts, and therefore will vary with age and Pb concentration. We have attempted to quantify the uncertainty by propagating error estimates (count statistical errors and calibration uncertainties) through a two-term Taylor expansion of the age equation. The results suggest that analytical precision is on the order of 5–10 my (1σ standard deviation) for an average of four analyses in relatively Pb-rich monazite (>2000 ppm) and nearer to 10–20 my for younger or Pb-poor monazite. These estimates ignore possible correlations of errors, which undoubtedly exist. A reasonable estimate of the precision for a single monazite age determination may come from

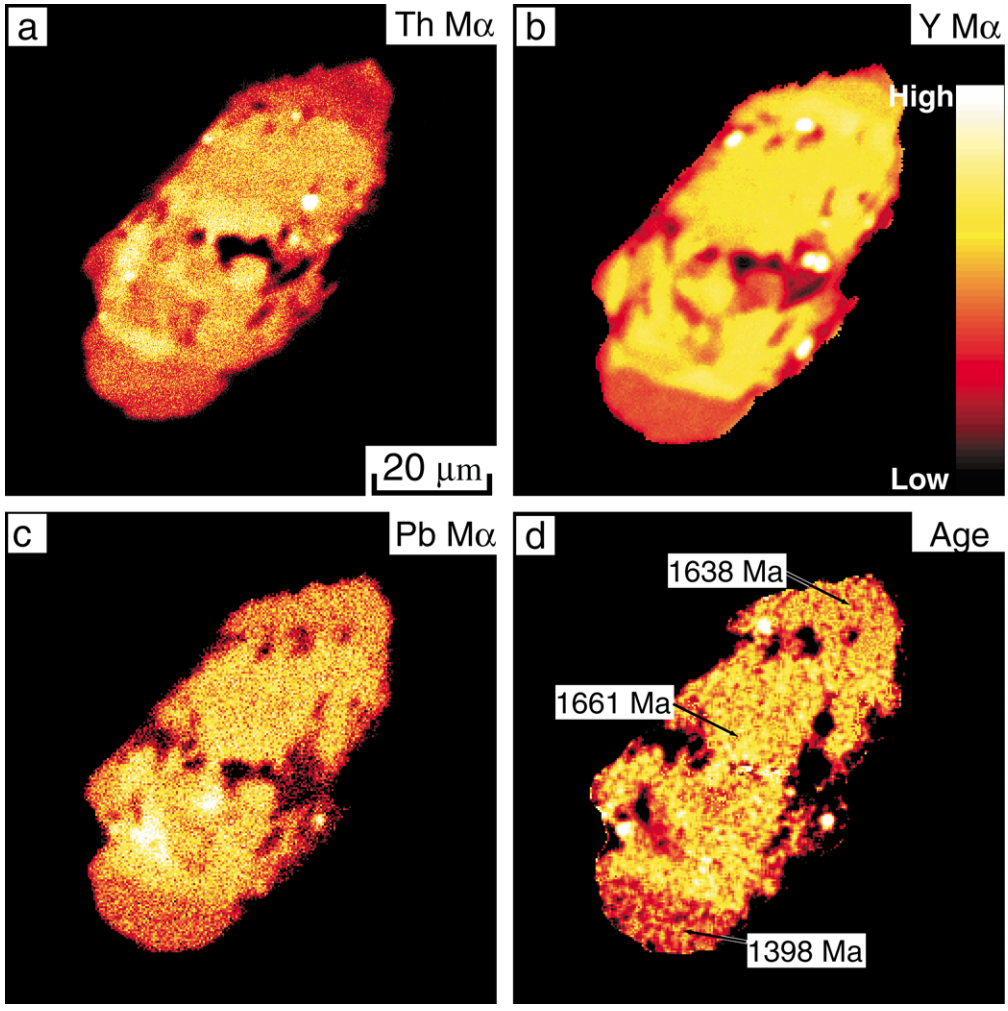

Fig. 3. High-resolution compositional images and 'age map' from a monazite crystal (HS12M3) from the Homestake shear zone, Colorado (Shaw et al., 2001). $Th_{M\alpha}$ (a), $Y_{L\alpha}$ (b), and $Pb_{M\alpha}$ (c) images were created simultaneously by holding the stage fixed and scanning the electron beam (current; 200 nA, count time; 500 ms/pixel, size;256 × 256 pixels). Note that relative intensities do not necessarily correlate. (d) Age map of the same crystal created by calculating a Th–U–Pb microprobe date for each pixel in the above maps (Williams et al., 1999a). Note that the two tips on the older core have distinctly different dates, 1638 vs. 1398 Ma.

calculating the standard error of the mean for a set of analyses taken within a mapped compositional subdomain. Typically, standard errors are very close to the propagated uncertainties, i.e. 5–10 my for relatively Pb-rich monazite. In several cases, larger standard errors have been obtained and are suspected to reflect compositional zonation or variation at a scale smaller than our spatial resolution, and in this regard, the magnitude of the standard error can be an indication of the homogeneity and stability of the domain being investigated. Preliminary attempts to characterize uncertainties using a Monte Carlo approach have yielded similar results (Arthur White, personal communication, 2000), and the relative convergence of propagated uncertainties, standard errors of the mean and Monte Carlo-based estimates give confidence that a precision of 5–10 my is reasonable in many cases. Of course, the accuracy of the analyses also depends on the quality of the standards, accuracy of the matrix algorithm, accuracy of physical constants associated with matrix effects, and on the degree to which the monazite has remained a closed system since its growth or recrystallization. Analyses of secondary standards and comparisons with monazite dates obtained by other methods suggest that the analyses are relatively accurate; they are generally consistent within the estimated precision, but no attempts have been made to quantify the total uncertainty (precision plus accuracy). In fact, for evaluating the nature and number of tectonic events, the precision may be the more important value.

4. Results

Microprobe age mapping and dating, because of their rapid and inexpensive nature, can be efficient reconnaissance tools for evaluating metamorphic and deformational age domains in large or poorly constrained areas. This sort

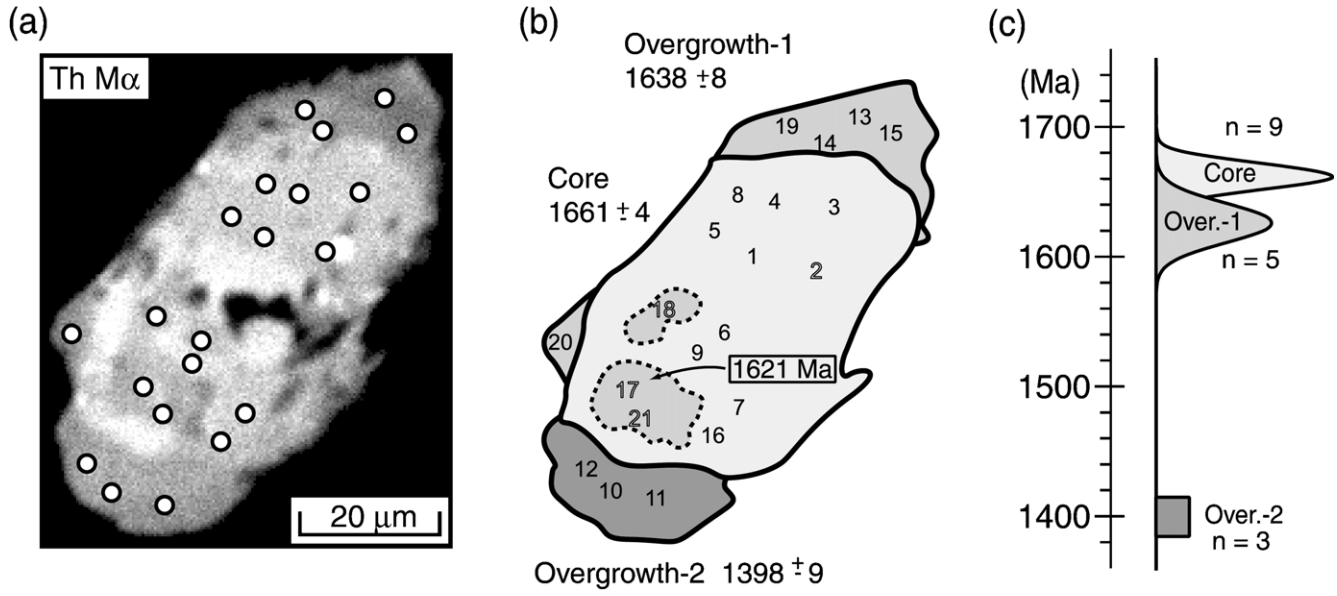

Fig. 4. (a) $Th_{M\alpha}$ compositional map of monazite HS12M3 (see Fig. 3) from the Homestake shear zone, Colorado with analysis points superimposed. Locations of analytical points are obtained by tracing the outline of the monazite grain and the point locations from a backscatter image, and then superimposing the tracing over the $Th_{M\alpha}$ map. (b) Point numbers and interpreted domains. Note: point-2 was excluded because it fell partially on a ThO2 inclusion. Point 18 was excluded because it fell on a Pb-rich inclusion. Points 17 and 21 were also excluded. They occur in distinct compositional domains interpreted to be related to Overgrowth-1. (c) Normalized distribution diagram showing mean and 1σ standard errors for monazite domains. These sorts of diagrams allow results from different monazite crystals to be compared and relative significance of internal domains to be evaluated.

of reconnaissance monazite dating is being conducted as part of regional mapping and tectonic analysis of the Western Churchill Province, Canada. This is allowing us to map out the fundamental domains of >3000, 2600, and 1900–1800 Ma tectonism and to identify the most important tectonic boundaries (Williams et al., 2000). However, microprobe monazite dating is much more than a reconnaissance tool. Because of its in-situ nature, its high spatial resolution, and rapid element mapping capability, the microprobe can provide insight not obtainable by other geochronologic methods, especially when integrated into detailed microstructural and micro-metamorphic studies. The main purpose of the examples below is to demonstrate the power of the integration of microstructural analysis and microprobe geochronology. Three specific types of applications will be highlighted: (1) timing of metamorphic events; (2) timing of deformational events; and (3) providing insight into conventional high-resolution geochronologic data. One important initial result from our monazite search procedure is the recognition that monazite, particularly fine-grained monazite (5–20 μ), is extremely common in rocks of a wide range of compositions, from mafic to felsic, allowing age constraints to be obtained from a majority of rocks in a study area. These fine-grained monazite crystals would not be captured by most conventional separation techniques (S.A. Bowring, personal communication, 2000).

4.1. Timing metamorphic events

Monazite inclusions in metamorphic porphyroblasts can be used to put specific time constraints on *P–T* paths and they can help to distinguish the effects of superimposed metamorphic pulses or cycles. For example, rocks in the Neil Bay area of northern Saskatchewan occur just west of the Snowbird zone, the boundary between the Rae and Hearne provinces of the Canadian Shield (Hanmer, 1997; Kopf, 1999). In order to understand the tectonic significance of the Snowbird zone, the age of metamorphism and deformation in the 'wall rocks', and particularly, the time of exhumation, must be understood. Phase relationships at Neil Bay indicate a relatively typical, clockwise *P–T* path involving granulite facies metamorphism followed by exhumation (Fig. 5) (Kopf, 1999). Garnet grew during high *P–T* biotite dehydration melting. Cordierite, biotite, and sillimanite developed during exhumation. Monazite occurs as an inclusion mineral in most metamorphic porphyroblasts and most of the monazite crystals contain at least two age domains (Fig. 5). Four distinct monazite growth events have been documented and correlated across the region: 1910, 1880, 1840, and 1800 Ma, in addition to local remnants of even older monazite. The older two regionally correlative dates (1910 and 1880 Ma) come from monazite inclusions in garnet. Monazite inclusions in cordierite yield 1840 Ma dates, but most cordierite has extensive pinite alteration and it is not certain that monazite inclusions were present before alteration. Matrix monazite crystals associated with sillimanite and biotite have 1800 Ma rims and cores of one or more of the older age populations (Fig. 5b). Taken together the data suggest that high-*P–T* melting and garnet growth occurred after 1910 Ma and before

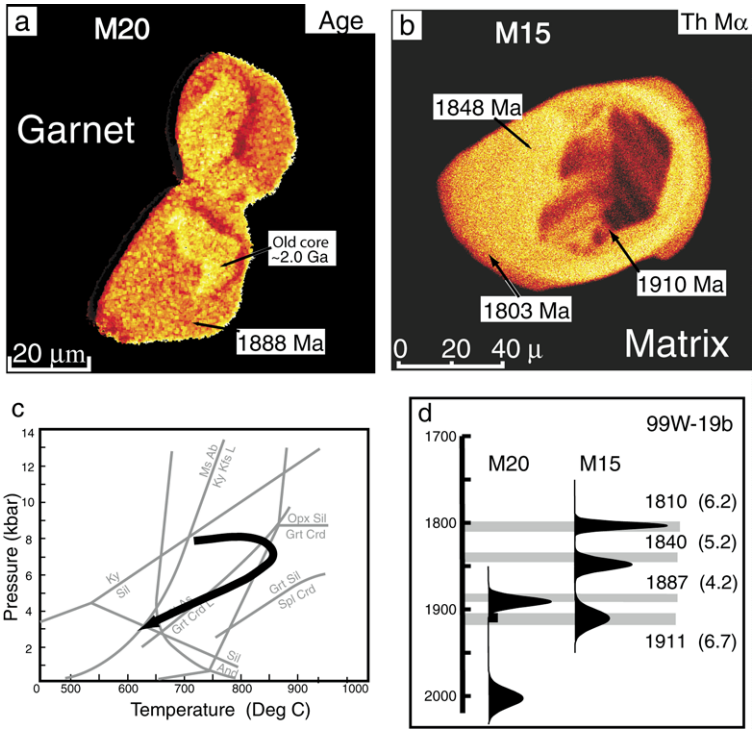

Fig. 5. Timing exhumation in the Neil bay area, Northern Saskatchewan (after Kopf, 1999). (a) Age map of monazite inclusions in garnet and (b) $Th_{M\alpha}$ compositional image of matrix monazite both from sample 99W19b. (c) Interpreted P–T path, based on thermobarometry and phase equilibria (Kopf, 1999), abbreviations after Kretz (1983). (d) Monazite dates from grains M15 and M20 (above). Gray bars and labels show weighted means and standard deviation (1σ) from eight monazite crystals in sample 19b (two of which are shown above). Monazite inclusions in garnet contain only the two older age populations and isolated older core domains.

1840 Ma. Decompression and cordierite growth occurred after 1840 Ma, and the final stages of tectonism and annealing occurred at approximately 1800 Ma. This is an extremely important result. First, the long duration of metamorphism and tectonism (1900–1800 Ma) may correspond to two different reactivation events, perhaps associated with collision of the Slave province to the NW (~1900 Ma) and later the Superior province to the SE (1840–1800 Ma) (Hoffman, 1989). Second, because these events apparently correspond to the time of annealing of much of the region, the data indicate that rocks of the Snowbird zone may have resided in the deep crust for hundreds of millions of years before exhumation (Williams et al., 2000).

A second example comes from rocks of the upper granite gorge of the Grand Canyon, Arizona. Rocks in this part of the Grand Canyon were metamorphosed primarily during the 1700–1650 Ma Yavapai orogeny (Hawkins et al., 1996; Ilg et al., 1996), the major period of Proterozoic continent accretion in the region. The 1840 Ma Elves Chasm gneiss represents the oldest rock yet recognized in the Southwest. Metamorphic rocks near the margin of the gneiss contain a number of distinctive assemblages including a coarse garnet + leucosome gneiss (migmatite) that contrasts sharply with turbiditic schists further from the pluton. The presence of the garnet migmatites near all exposed contacts might suggest that metamorphic grade increases toward the pluton, i.e. contact metamorphism. This, in turn, implies that the assemblages may represent an older (1840 Ma) metamorphic event and that older country rocks may be present near the gneiss. However, Bowring and Hawkins (personal communication) have recognized 1700–1750 Ma detrital zircon in schists near the gneiss indicating that the gneiss is in contact with significantly younger rocks.

Fig. 2 shows a full-section Mg and Ce map from the garnet gneiss adjacent to the Elves Chasm pluton. The large garnet crystal and the adjacent leucosome (dark area on map) are interpreted to have developed during biotite dehydration melting. Monazite inclusions in the garnet crystal tend to be small and anhedral in shape (Fig. 6a). Several of the inclusions have two age domains, with dates of: ca. 1750 Ma for the core and ca. 1700 Ma for the rims (Fig. 6b). The internal domain boundaries are cut by the inclusion grain boundaries suggesting that larger grains may have been dissolved or eroded. One monazite inclusion within a quartz inclusion in the garnet yields a ca. 1900 Ma date (see below). Matrix monazite grains commonly occur within or adjacent to biotite. They are larger and more euhedral than the inclusion grains (Fig. 6c), and most of the grains are distinctly cracked and broken. Although many matrix grains are altered or weathered, they yield consistent 1660–1680 Ma dates, typical of monazite throughout the Grand Canyon (Hawkins, 1996; Hawkins et al., 1996). The

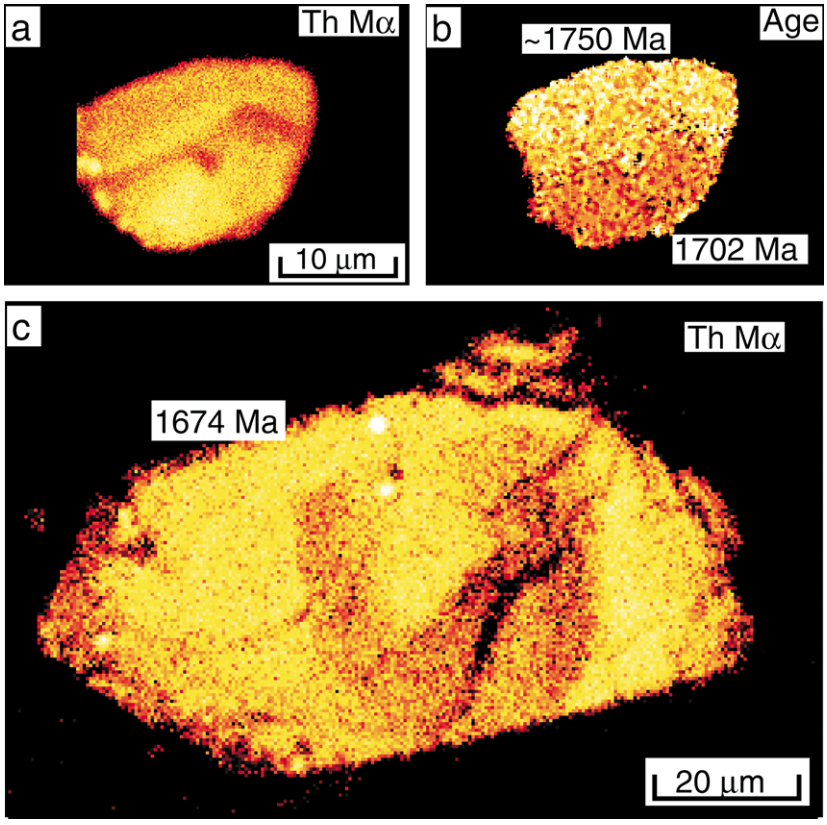

Fig. 6. Timing high-*T* metamorphism near the 1840 Ma Elves Chasm pluton, Upper Granite Gorge, Grand Canyon. $Th_{M\alpha}$ (a) and age map (b) of monazite inclusion in large garnet porphyroblast shown in Fig. 2. The grain shows two age domains, typical of most inclusion grains. (c) $Th_{M\alpha}$ compositional map of matrix grain from same sample. Age map shows little age variation. Crystal is subhedral and aligned in the dominant foliation.

presence of 1750 and 1700 Ma dates within garnet indicates that the distinctive metamorphic assemblages and textures (garnet + leucosome) do not represent an older stage of metamorphism, but instead are synchronous with the Yavapai metamorphism in the Grand Canyon. The border zone to the Elves Chasm gneiss may represent a weathered zone (regolith) on the older basement that had a particularly appropriate composition for melting reactions. The presence of ca. 1900 Ma monazite and the 1750 Ma domains, the age of early volcanism, suggest that detrital monazite grains were present in this soil horizon. It is possible that some increase in metamorphic conditions may in fact have occurred near the older pluton due to conductivity and heat production contrasts between the pluton and its country rocks, but the monazite data preclude any syn-plutonic heating and thus, refocus the questions to be asked at this locality.

The final example comes from Proterozoic rocks of northern New Mexico. This region is well known for the widespread exposure of amphibolite facies rocks that crystallized near the Al-silicate triple point (Grambling, 1981; Grambling and Williams, 1985). The amphibolite facies metamorphism was long interpreted to be associated with the 1650 Ma Mazatzal orogeny, although Grambling suggested that some of the 'triple point' exposures could be younger (ca. 1400 Ma) based on Ar–Ar geochronology (Grambling and Dallmeyer, 1993; Karlstrom et al., 1997). Although the effects of 1400 Ma metamorphism and deformation have been increasingly recognized in the southwestern USA, most rocks are characterized by multiple *P–T* loops and the age (or ages) of the regional amphibolite facies metamorphism has not been clear (see Fig. 1). Fig. 7 shows a large staurolite porphyroblast from the Cerro Colorado area of northern New Mexico, an area that contains kyanite, andalusite, and sillimanite (Bishop, 1997; Williams et al., 1999b). Monazite inclusions have been found in staurolite, kyanite, and andalusite and all are ca. 1400 Ma. Although it remains possible that some of the older metamorphic loops occurred during the Yavapai/Mazatzal orogeny, the youngest event (that associated with most aluminum silicates) occurred during the 1400 Ma heating and reactivation. Nearly identical assemblages and textures in other parts of the region (i.e. the Upper Gorge of the Grand Canyon) were developed during the 1660–1680 Ma orogenesis. Microprobe monazite geochronology provides an efficient way to map the exposures of ca. 1680 and ca. 1400 Ma metamorphic domains, a major first step in understanding the controls on the character of orogenesis and the controls on reactivation 200 my after the initial orogeny.

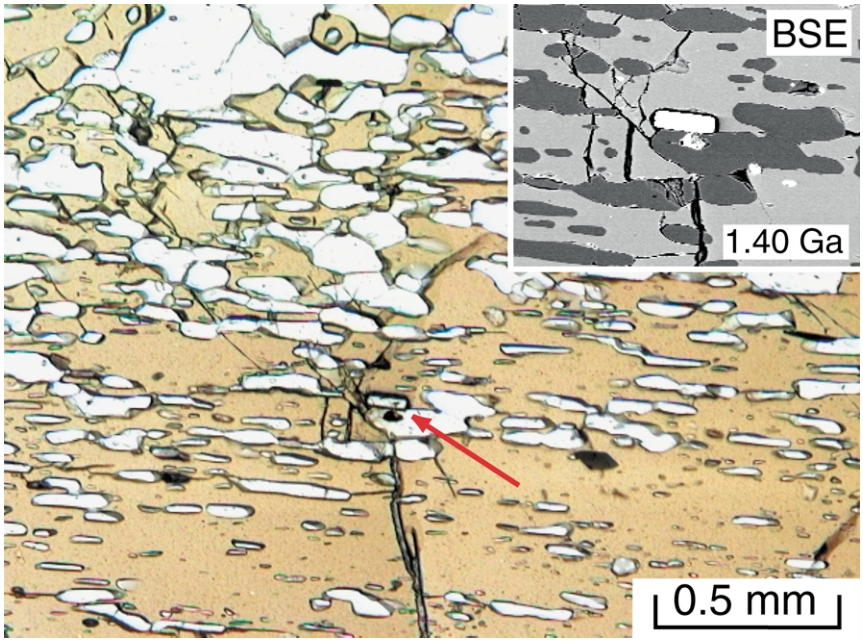

Fig. 7. Photomicrograph and backscattered electron image of a monazite inclusion in Staurolite, Cerro Colorado area, northern New Mexico. Monazite in staurolite, kyanite and andalusite crystals all give relatively homogeneous 1400 Ma dates indicating that the regional triple point metamorphism is associated with 1400 Ma reactivation, not the 1650–1700 Ma Yavapai or Mazatzal orogenies. Red arrow points to monazite inclusion and to area of insert. Modified from Williams et al. (1999a).

4.2. Timing deformation events

Because monazite is commonly a fabric forming and inclusion bearing mineral, microfabrics and microtextures associated with monazite can help to constrain the age of deformation events and provide new links between metamorphism and deformation. In some cases, monazite textures can be directly tied to deformation fabrics and textures. For example, some monazite crystals from the Homestake shear zone of Colorado have been offset by fractures associated with an event of dip-slip shearing (Fig. 8) (Shaw et al., 2001). In other cases, monazite overgrowths occur in distinctive locations, asymmetries, or geometries that can be interpreted with respect to tectonic fabrics. Fig. 9 shows a large monazite crystal from a relatively late dextral *S–C* mylonite zone near the margin of the East Athabasca mylonite triangle in Saskatchewan. Although the core of the grain yields 2400 Ma dates, a

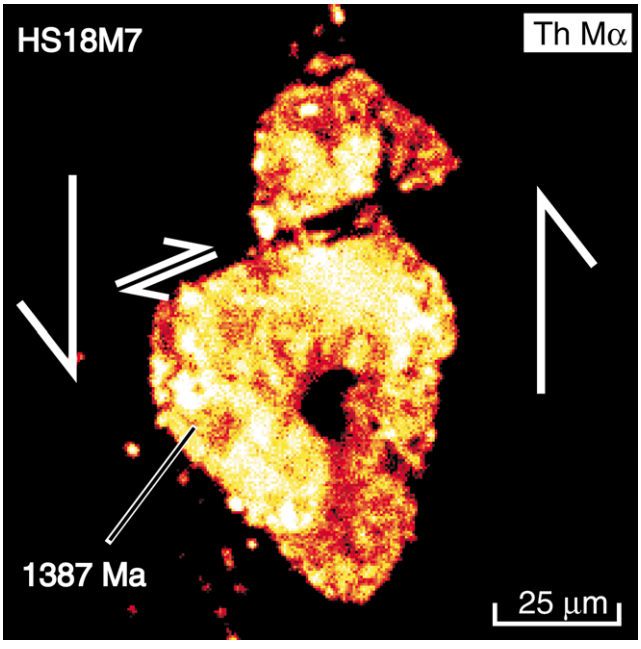

Fig. 8. $Th_{M\alpha}$ compositional map of matrix monazite grain from Homestake shear zone, Colorado (after Shaw et al., 2001). Fractures in grain are compatible with fractures observed in outcrop and with kinematics of low-*T* shearing (see Shaw et al. (2001) for discussion).

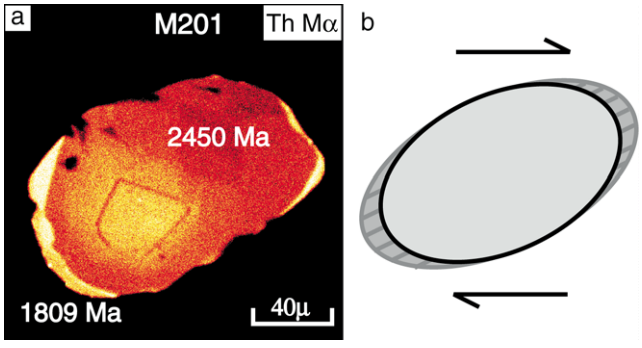

Fig. 9. $Th_{M\alpha}$ compositional map (a) and interpretation (b) of a monazite grain from a late shear zone near the margin of the East Athabasca mylonite triangle, northern Saskatchewan. Late dextral shearing is associated with overgrowths on older monazite, constraining the late shearing event to approximately 1805 Ma.

distinct set of high-Th overgrowths were preferentially developed in the extensional quadrants associated with dextral shear. These yield consistent 1810–1800 Ma dates suggesting that a component of relatively late-stage dextral strain occurred along the edge of the East Athabasca mylonite triangle.

Monazite overgrowths are commonly aligned with mineral lineations or foliations. The interpretation of these textures is somewhat more equivocal, and requires a better understanding of how deformation influences mineral growth, but important timing constraints can generally be extracted. For example, a monazite crystal from the Homestake shear zone, Colorado (Shaw et al., 2001), has overgrowths that were developed at two separate times, ca. 1638 and 1398 Ma (Figs. 3 and 4). The overgrowths occur on opposite ends of the crystal and are aligned with the mineral lineation. We interpret these overgrowths to represent shearing events, when matrix minerals were separated (extended) from the monazite core, allowing access of fluids to the crystal. These overgrowths appear to record times of reactivation in the Homestake shear zone. With regard to monazite geochronology in general, it is interesting to note that several compositionally distinct domains within the monazite crystal yield dates that are indistinguishable from the older overgrowth (Fig. 4b). We suspect that these domains are embayments in the monazite core that were infilled during the overgrowth event. These small domains, if unrecognized, could compromise the results from most other analytical techniques.

Although structurally-controlled or fractured monazite crystals are particularly notable, more commonly, constraints on the timing of deformation events come from monazite inclusion relationships in other porphyroblasts. Proterozoic rocks from northern New Mexico are a typical example. As noted above, a broad array of data, including results of microprobe monazite geochronology, have indicated that a significant metamorphic event occurred in association with the widespread 1450–1350 Ma granitic plutonism across the Southwest. Because of the generally small amount of internal deformational fabric, many of these granitoids have been called ‘anorogenic’. However, significant amounts of deformation have been interpreted in several areas (Nyman et al. 1994; Duebendorfer and Christensen, 1995; Kirby et al., 1995), and it is critical to assess the amount and nature of the deformation associated with this regional plutonism.

Fig. 10a is a sketch of a garnet porphyroblast included within a large staurolite porphyroblast from the Cerro Colorado area of the Tusas Mountains, New Mexico. The staurolite crystal has overgrown the dominant regional foliation (S2b). Outside of the staurolite, this foliation is folded into a series of kilometer-scale upright folds with moderately developed axial plane foliation (S3). The garnet crystal contains two texturally and compositionally distinct domains, core and rim (Bishop, 1997). The core contains an early sigmoid-style inclusion trail (S1), that is truncated by (and locally curves into) a rim fabric (S2a). The garnet rim fabric (S2a) curves smoothly through an angle of approximately 30° into the typical staurolite inclusion fabric (S2b). The two foliations (garnet rim and staurolite inclusion fabric) are similar in style but differ in orientation, and the angular relationship is maintained from porphyroblast to porphyroblast in a number of samples. Subhedral to euhedral monazite inclusions are relatively abundant in staurolite (see Fig. 7), and yield consistent ca. 1400 Ma dates. This suggests that the staurolite is younger than 1400 Ma, but does not necessarily constrain the age of deformation. However, a small monazite inclusion (M8) from the overgrowth region of the included garnet also yielded a 1400 Ma date. In addition, a monazite inclusion in staurolite just outside of the garnet crystal (Fig. 10, Monazite-9) yielded dates of 1670 Ga (core) and 1400 Ma (rim).

The interpretation of these data depend upon the interpretation of the microstructures themselves. We suggest that the consistency of the S2a orientation from sample to sample indicates that S2a and S2b are distinct fabrics, and that S2a has been reactivated (Bell, 1986) at a later time by S2b. If so, then the dominant reactivated fabric across the region (S2b) developed after 1400 Ma. This suggests a significant amount of deformation associated with the 1400 Ma thermal event. Alternatively, the angular relationship between S2a and S2b might represent a single fabric anastomosing around garnet porphyroblasts, in this case the garnet core, and thus the 1400 Ma dates may not constrain the age of S2, but only the timing of the garnet rims and the staurolite host. The S2 fabric could potentially be older. So far, no monazite inclusions have been found in the garnet core region or in any other preserved S1 domain. Because 1400 Ma monazite is extremely abundant throughout the region, we take this as evidence that the S1 fabric may indeed be older. Typical of many such specific microstructural problems, it may be necessary to prepare a number of thin sections in order to find a monazite grain in a critical microstructural setting. The presence of the 1670 Ma date from the core of monazite M9 indicates that some early monazite crystals were present in the rocks and thus, additional thin sections through this or similar rocks could potentially yield a critical constraint on the age of the earliest fabrics.

4.3. Interpreting companion geochronologic data

Age mapping and dating can provide insight into complex results from other geochronologic techniques. This is illustrated in each of the examples presented above, but one additional example is particularly telling. Previous monazite dates from the Lower Gorge of the Grand Canyon (Fig. 11) tend to spread over several tens of millions of years (1690–ca. 1650 Ma), even though most are nearly concordant (Davidek et al., 1998). Age mapping reveals that most monazite grains have a euhedral core domain that is ca.

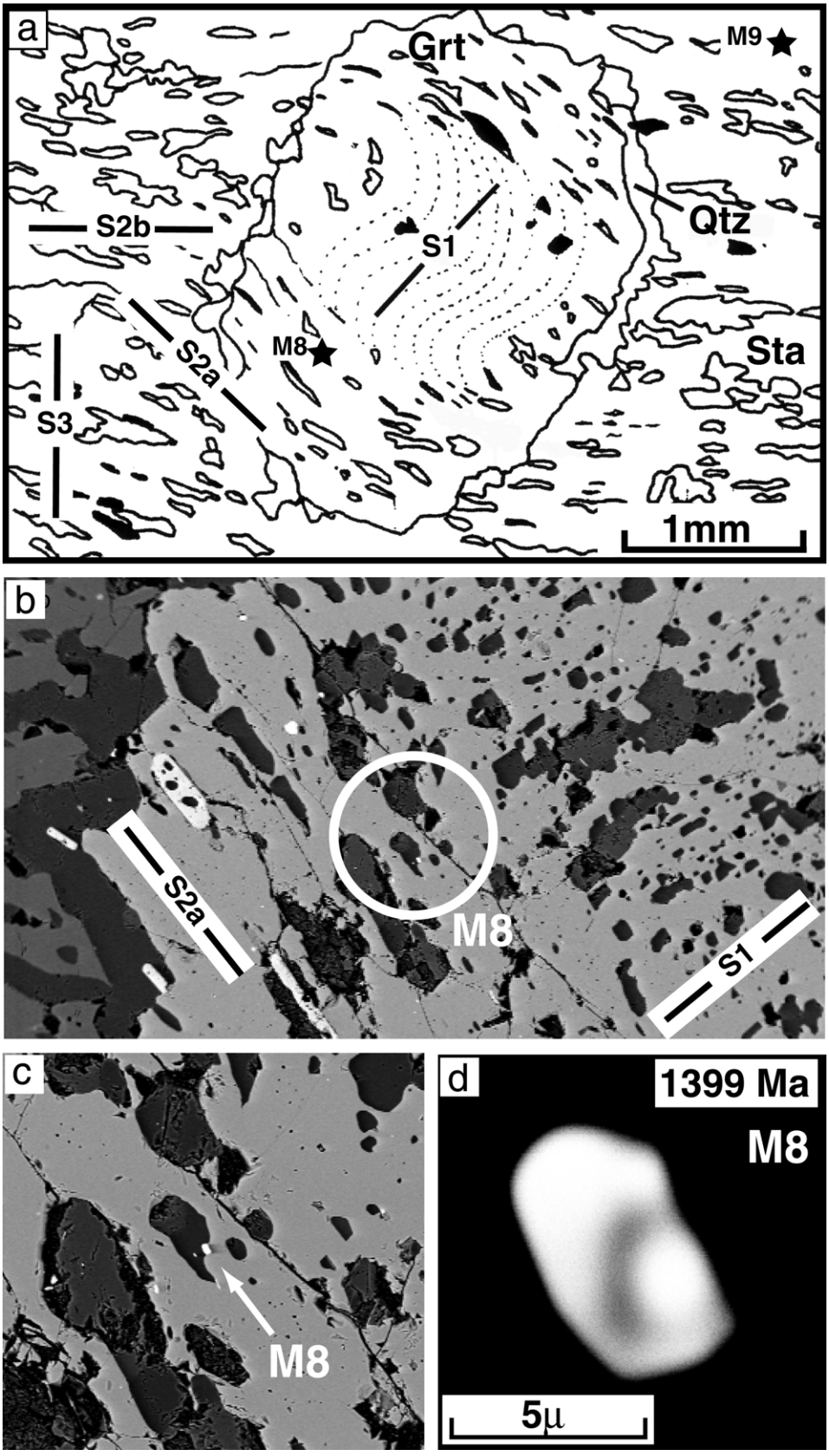

Fig. 10. Microstructural relationships in sample JB56b from the Cerro Colorado area, northern New Mexico. (a) Sketch of inclusion patterns in a garnet porphyroblast that is included in a large staurolite porphyroblast. (b) Backscattered electron image of part of garnet inclusion. Circle shows the location of monazite inclusion (c,d). See text for discussion.

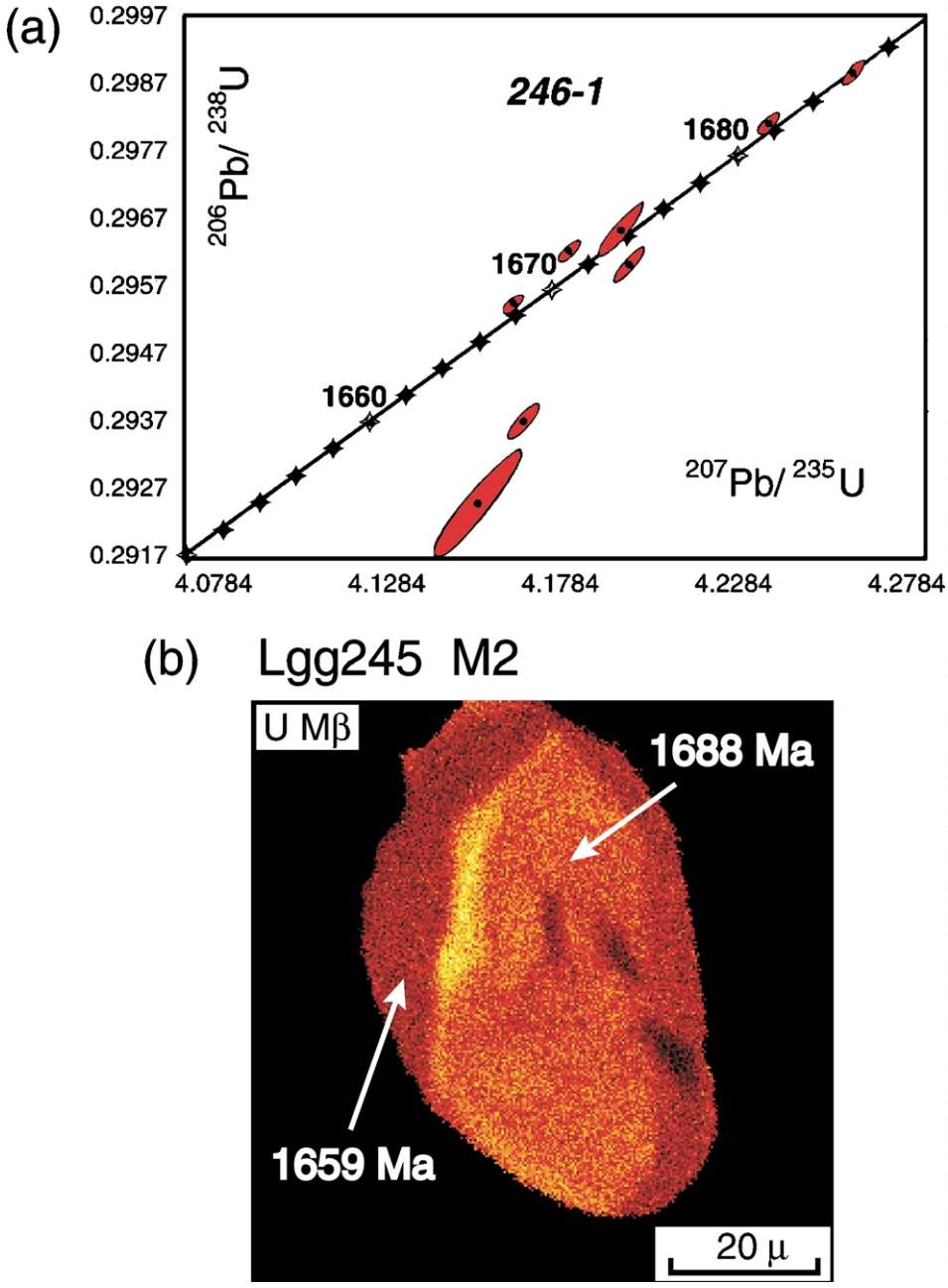

Fig. 11. Geochronologic data from monazite from mile 246 of the Lower Granite Gorge of the Grand Canyon (a) Concordia diagram showing U–Pb TIMMS monazite data (Keefe and Bowring, personal communication, 2000). Note spread of intercept dates from ca. 1690 to ca. 1670 Ma. (b) $U_{M\beta}$ compositional map of a single monazite grain from approximately 0.75 km from above geochronology sample. Note that the grain has a typical round exterior but contains a euhedral internal crystal form. Microprobe dates from the internal crystals are tightly clustered at 1688 Ma. Anatexis is interpreted to have occurred at 1688 Ma; overgrowths developed at a variety of times from ca. 1670 to 1640 Ma.

1690 Ma with overgrowths ranging from 1670 to 1640 Ma (Fig. 11b). Even single-crystal whole-monazite dates have undoubtedly yielded an average of these domains. Although more work is needed on the petrologic and mechanical controls on monazite growth, particularly on the implications of euhedral vs. anhedral crystals, we suggest that the euhedral core represents the time of migmatization, or more specifically, monazite growth during melt crystallization (Pyle and Speer, 2000). The anhedral overgrowths are interpreted to represent subsequent thermal or hydrothermal events during slow, isobaric cooling. The spread of nearly concordant monazite dates are almost certainly mixtures of core and rim domains.

Finally, from a procedural point of view, the monazite core domains are defined solely by U compositional variation. They are essentially invisible on backscattered electron

images. This underscores the need for compositional mapping rather than electron imaging to characterize monazite domains.

5. Discussion and conclusions

The general conclusion of our work so far is that monazite age mapping and dating on the microprobe allow geochronology to be an integral part of the microstructural analytical process rather than a subsequent activity. Accurate dates (ages) can be obtained directly from within a microstructure or microtexture under investigation, providing a new means of developing and testing hypotheses during the analytical process. Further, dates can be obtained from a large number of samples rather than a small subset. Informed decisions can be made about which samples require high-precision isotopic analysis, and the results of those analyses can be better integrated with all other petrologic and structural data. High resolution compositional mapping is an essential component of microprobe dating. Virtually all monazite crystals that we have investigated are compositionally zoned, and the overwhelming majority have some age zoning. The geometry of compositional and age domains is an important microstructural element that can tie the monazite dates into metamorphic or structural processes, but careful analytical methods are critical. Large scatter or meaningless data can result from microprobe analyses that overlap compositional or age domain boundaries.

Most regions that we have investigated in the Canadian Shield or in the southwestern USA contain monazite with more than one age domain. The geometry of these domains can be quite complex with rims developed on only one edge of a core or isolated embayments in older cores, filled by a younger generation. These could not be adequately investigated by simple abrasion techniques. Also, if the rims do not involve a significantly different Th composition, they would not necessarily be apparent on backscattered electron images, and many are too narrow to be analyzed by current ion beam or laser techniques. The electron microprobe is the only tool with sufficient spatial resolution to investigate these complex grains.

Several general conclusions from our two primary study areas are relevant to microstructural analysis and to tectonic processes and geochronology in general. In both field areas, similar metamorphic grades and similar deformational fabrics have been developed at very different times and in different tectonic settings. This may be particularly common in regions characterized by isobaric cooling: those that experience a tectonic event and then cool at some level in the crust (Williams and Karlstrom, 1996; Williams et al., 1999b, 2000). Such regions are susceptible to later tectonic (heating) events and could develop new assemblages and structures at similar pressures to those at which the terrane cooled. Parts of the southwestern USA reached amphibolite facies conditions during the 1650–1700 Ma Yavapai/Mazatzal orogeny and again during the 1400 Ma reactivation. Archean rocks in northern Saskatchewan reached granulite facies conditions at 2600 Ma during transcurrent shearing and again at 1900 Ma associated with reactivation and exhumation. In both areas, tectonic models critically depend on distinguishing the minerals and structures that developed during these disparate events. Microprobe monazite chronology has proven to be an ideal tool for constraining the absolute ages of these events.

Although our original goal was to use microprobe monazite dating as a reconnaissance tool to distinguish events widely spaced in time, the technique has proven to be sufficiently precise to add insight into the stages within tectonic events. In the southwestern USA, we have been able to distinguish several stages in both the 1650–1700 Ma and ca. 1400 Ma events (Figs. 3 and 9; see also Shaw et al., 2001). In northern Saskatchewan, the general 1900–1800 Ma deformation/metamorphic event involved pulses of monazite growth at four distinct times, 1910, 1880, 1840 and 1800 Ma, and deformation at two times, at least, before and after 1840 Ma. In these and in several other areas in which we have applied the monazite technique, the general 80–100 my tectonic cycle involves pulses of monazite growth with time spans in the order of 10 my or shorter. We suspect that deformational pulses might lead to fluid influx and dissolution or growth of monazite. Microprobe monazite geochronology, when carefully applied, has the resolution to map and characterize the spatial and temporal subdomains within tectonic events.

The examples presented above illustrate the strengths and limitations of microprobe monazite dating, as we currently understand it, for constraining the timing of metamorphism and deformation. The most ideal situation would be to directly determine the structural, and petrological (or geochemical) controls on monazite growth, so that a monazite growth event would have immediate *P–T–D* significance. That is, the monazite growth event itself could be placed on the *P–T–D* path and provide its own time constraint. Although some progress has been made in investigating monazite petrology and geochemistry (Pyle and Speer, 1999, 2000; Rubatto et al., 2001), the fact that there can be numerous monazite growth events within a single tectonic cycle suggests that multiple reactions and growth mechanisms may be involved, perhaps including a combination of mineral reactions and fluid influx events. In the absence of clear monazite phase relationships, it is generally necessary to use inclusion relationships to draw firm conclusions about timing. Samples must be carefully selected based on microstructural constraints, and then multiple polished sections must be prepared until a monazite crystal, appropriately located to place constraints on critical questions, can be found. Typically, important conclusions can be immediately drawn from matrix monazite or the most abundant population of monazite inclusions. For example, the age of the youngest garnet

and staurolite assemblage and the locally important S3 cleavage in Fig. 10 are both post-1400 Ma. Much more careful work may be required to constrain the age of older and more subtle fabrics (i.e. S1 and S2; Fig. 10). In fact, monazite geochronology brings renewed pressure and justification for detailed microstructural analysis because with it, a better understanding of the significance of inclusion trail geometries and of mineral inclusions themselves can yield important age constraints on regional deformation events. In many ways, monazite can be thought of as providing a set of time markers with which other aspects of microstructure and microtexture must be linked.

Microprobe monazite geochronology offers no internal check on the accuracy of the calculated dates, such as concordance of Th–Pb and U–Pb systems, although the sharpness of compositional domain boundaries and the consistency of measurements can argue that a particular grain has not been significantly altered or modified. We have found that the microprobe technique may be at its most powerful when combined with other geochronologic methods such as U–Pb TIMS analyses of monazite and zircon. These conventional techniques can establish some of the basic geochronologic constraints such as crystallization ages of igneous rocks and bulk ages of monazite, titanite, apatite, and other chronometer phases. Then, within these parameters, microprobe mapping and dating can place constraints on the age of fabrics and textures and thus on *P–T–D* history. In this respect, microprobe monazite chronology is a powerful companion for conventional techniques. In the future, much more along these lines might be done to use microprobe mapping to place other chronometer phases into compositional and microstructural context.

Future research certainly will enhance the power and breadth of microprobe monazite geochronology as a tool for microstructural and tectonic analysis. Important research directions include: analysis of phase relationships and geochemical controls on monazite growth and dissolution, analysis of monazite crystal chemistry and the possible factors that can lead to Pb diffusion or leaching, analysis of microstructures and the dynamics of entrapment and preservation of mineral inclusions, and importantly, analytical developments that will reduce detection limits and analytical uncertainty and also allow increased spatial resolution during mapping. Further application and refinement of the technique will allow conclusions to be drawn not only about older or long-lived orogenic events, but increasingly about the rates of typical metamorphic and tectonic processes and detailed synchroneity of events across orogenic belts.

Acknowledgements

Partial financial support for this research was provided by NSF Grants EAR-9909421 and EAR-0001152 supporting research in the southwestern USA and Canadian Shield, respectively. The authors sincerely thank Paul Karabinos and Art Goldstein for helpful and constructive reviews and Sheila Seaman for valuable comments on an earlier draft of this manuscript. The authors also thank Liane Stevens for operating the electron microprobe for several of the maps and analyses presented above.

References

Anderson, J.L., 1989. Proterozoic anorogenic granites of the southwestern United States. In: Jenny, J.P., Reynolds, S.J. (Eds.). Geologic Evolution of Arizona, vol. 17. Arizona Geological Society, Tucson, pp. 211–238.

Bell, T.H., 1986. Foliation development and refraction in metamorphic rocks: reactivation of earlier foliations and decrenulation due to shifting patterns of deformation partitioning. Journal of Metamorphic Geology 4, 421–444.

Bishop, J.L., 1997. The determination of a quantitative *P–T–t–D* history for Proterozoic rocks of the Cerro Colorado area, north central New Mexico. M.S. thesis, University of Massachusetts.

Bosbyshell, H., Jercinovic, M.J., 1999. Electron microprobe age determinations in the Wissahickon Fm. of SE Pennsylvania. Geological Society of America Abstracts with Programs 31.

Cherniak, D.J., Watson, E.B., Harrison, T.M., Grove, M., 2000. Pb diffusion in monazite: a progress report on a combined RBS/SIMS study. EOS Supplement, S25.

Cocherie, A., Legendre, O., Peucat, J.J., Kouamelan, A., 1998. Geochronology of polygenetic monazites constrained by in situ electron microprobe Th–U–Total Pb determination: implications for Pb behavior in monazite. Geochimica et Cosmochimica Acta 62, 2475–2497.

Crowley, J.L., Ghent, E.D., 1999. An electron microprobe study of the U–Th–Pb systematics of metamorphosed monazite: the role of Pb diffusion versus overgrowth recrystallization. Chemical Geology 157, 285–302.

Daniel, C.G., Karlstrom, K.E., Williams, M.L., Pedrick, J.N., 1995. The reconstruction of a middle Proterozoic orogenic belt in north-central New Mexico, USA. New Mexico Geological Society Guidebook, 46th Field Conference, pp. 193–200.

Davidek, K.L., Bowring, S.A., Karlstrom, K.E., Williams, M.L., Hawkins, D.P., 1998. Geochronological, thermochronological, and geological constraints on Proterozoic midcrustal suturing in the western Grand Canyon, Arizona. Geological Society of America Abstracts with Programs 30, 160.

Duebendorfer, E.M., Christensen, C., 1995. Synkinematic (?) intrusion of the "anorogenic" 1425 Ma Beer Bottle Pass pluton, southern Nevada. Tectonics 14, 168–184.

Grambling, J.A., 1981. Kyanite, andalusite, sillimante, and related mineral assemblages in the Truchas Peaks region, New Mexico. American Mineralogist 66, 702–722.

Grambling, J.A., Williams, M.L., 1985. The effects of Fe and Mn on aluminum silicate phase relations in north-central New Mexico, USA. Journal of Petrology 26, 324–354.

Grambling, J.A., Dallmeyer, R.D., 1993. Tectonic evolution of Proterozoic rocks in the Cimarron Mountains, northern New Mexico. Journal of Metamorphic Geology 11, 739–755.

Hanchar, J.M., Logan, A.M., Vicenzi, E.P., Thibault, Y., Stern, R., 2000. Electron microprobe dating of monazite: An assessment of precision and accuracy of the method. EOS Supplement, S26.

Hanmer, S., 1997. Geology of the Striding–Athabasca mylonite zone, northern Saskatchewan and southeastern District of Mackenzie, Northwest Territories. Geological Survey of Canada Bulletin 501, 1–92.

Hawkins, D.P., 1996. U–Pb geochronological constraints on the tectonic and thermal evolution of Paleoproterozoic crust in the Grand Canyon, Arizona. Ph.D. thesis, Massachusetts Institute of Technology.

Hawkins, D.P., Bowring, S.A., Ilg, B., Karlstrom, K.E., Williams, M.L., 1996. U–Pb geochronological constraints on Paleoproterozoic crustal evolution, Upper Granite Gorge, Grand Canyon, Arizona. Geological Society of America Bulletin 108, 1167–1181.

Hoffman, P.F., 1989. Precambrian geology and tectonic history of North America. In: Bally, A.W., Palmer, A.R. (Eds.). The Geology of North America — An Overview. Geological Society of America, Boulder, CO, pp. 447–512.

Ilg, B., Karlstrom, K.E., Hawkins, D., Williams, M.L., 1996. Tectonic history of Paleoproterozoic rocks in the Grand Canyon, Arizona. Geological Society of America Bulletin 108, 1149–1166.

Jercinovic, M.J., Williams, M.L., 2000. Electron microprobe age mapping and dating of monazite: techniques and applications. In: Williams, D.B., Shimizu, R. (Eds.). Microbeam Analysis 2000. Institute of Physics, Bristol, pp. 439–440 Conference Series No. 165.

Karlstrom, K.E., Williams, M.L., 1995. The case for simultaneous deformation, metamorphism, and plutonism: an example from Proterozoic rocks in central Arizona. Journal of Structural Geology 17, 59–81.

Karlstrom, K.E., Williams, M.L., 1998. Heterogeneity of the middle crust: implications for strength of continental lithosphere. Geology 26, 815–818.

Karlstrom, K.E., Dallmeyer, D., Grambling, J.A., 1997. $^{40}Ar/^{39}Ar$ evidence for 1.4 Ga regional metamorphism in New Mexico: implications for thermal evolution of the lithosphere in Southwestern USA. Journal of Geology 105, 205–223.

Karlstrom, K.E., Åhäll, K., Harlan, S.S., Williams, M.L., McLelland, J., Geissman, J.W., 111, 5–30 2001. Long-lived (1.8–0.8 Ga) Cordilleran-type orogen in southern Laurentia, its extensions to Australia and Baltica, and implications for refining Rodinia. Precambrian Research.

Kirby, E., Karlstrom, K.E., Andronicos, C., 1995. Tectonic setting of the Sandia pluton: an orogenic 1.4 Ga granite in New Mexico. Tectonics 14, 185–201.

Kopf, C.F., 1999. Deformation, metamorphism, and magmatism in the East Athabasca Mylonite Triangle, northern Saskatchewan: implications for the Archean and Early Proterozoic crustal structure of the Canadian Shield. Ph.D. thesis, University of Massachusetts.

Kretz, R., 1983. Symbols for rock-forming minerals. American Mineralogist 68, 277–279.

Livi, K.J.T., Olsen, S.N., Alcock, J., Isachsen, C., Muller, P.D., 2000. Some successes and failures in application of EMPA to accessory monazite and zircon. EOS Supplement 81, S27.

Montel, J., Foret, S., Veschambre, M., Nicollet, C., Provost, A., 1996. Electron microprobe dating of monazite. Chemical Geology 131, 37–53.

Montel, J.M., Kornprobst, J., Vielzeuf, D., 2000. Preservation of old U–Th–Pb ages in shielded monazite: example from the Beni Bousera Hercynian kinzigites (Morocco). Journal of Metamorphic Geology 18, 335–342.

Nyman, M.W., Karlstrom, K.E., Kirby, E., Graubard, C.M., 1994. Mesoproterozoic contractional orogeny in western North America: evidence from ca. 1.4 Ga plutons. Geology 22, 901–904.

Parrish, R.R., 1990. U–Pb dating of monazite and its application to geological problems. Canadian Journal of Earth Sciences 27, 1435–1450.

Pouchou, J.L., Pichoir, F., 1984. A new model for quantitative X-ray microanalysis. Part I: application to the analysis of homogeneous samples. La Recherche Aerospatiale 3, 13–38.

Pouchou, J.L., Pichoir, F., 1985. "PAP" phi-rho-Z procedure for improved quantitative microanalysis. In: Armstrong, J.L. (Ed.). Microbeam Analysis. San Francisco Press Inc, San Francisco, pp. 104–106.

Pyle, J.M., Speer, F.S., 1999. Y zoning in garnet: coupling major and accessory phases during metamorphic reactions. Geological Materials Research 1, 1–49.

Pyle, J.M., Speer, F.S., 2000. Accessory phase paragenesis in low-*P* migmatites, Chesham Pond nappe, SE New Hampshire. Geological Society of America Abstracts with Programs 32, A297.

Rubatto, D., Williams, I.S., Buick, I.S., 2001. Zircon and monazite response to prograde metamorphism in the Reynolds Range, central Australia. Contributions to Mineralogy and Petrology 140, 458–468.

Schmitz, M.D., Bowring, S.A., 2000. The significance of U–Pb dates in lower crustal xenoliths from the southwestern margin of the Kaapvaal craton, southern Africa. Chemical Geology 172, 59–76.

Shaw, C.A., Karlstrom, K.E., Williams, M.L., Jercinovic, M.J., McCoy, A.M., 2001. Electron microprobe monazite dating of ca. 1.7–1.63 and ca. 1.45–1.38 Ga deformation in the Homestake Shear Zone, Colorado: origin and evolution of a persistent intracontinental tectonic zone. Geology 29, 739–742.

Suzuki, K., Adachi, M., 1991. Precambrian provenance and Silurian metamorphism of the Tsunosawa paragneiss in the South Kitakami terrane, Northeast Japan, revealed by the chemical Th–U–total Pb isochron ages of monazite, zircon and xenotime. Journal of Geochemistry 25, 357–376.

Suzuki, K., Adachi, M., 1998. Denudation history of the high *T*/*P* Ryoke metamorphic belt, southwest Japan: constraints from CHIME monazite ages of gneisses and granitoids. Journal of Metamorphic Geology 16, 23–37.

Suzuki, K., Adachi, M., Kajizuka, I., 1994. Electron microprobe observations of Pb diffusion in metamorphosed detrital monazites. Earth and Planetary Science Letters 128, 391–405.

Terry, M.P., Robinson, P., Hamilton, M.A., Jercinovic, M.J., 2000. Monazite geochronology of UHP and HP metamorphism, deformation, and exhumation, Nordøyane, Western Gneiss Region, Norway. American Mineralogist 85, 1651–1664.

Williams, M.L., Karlstrom, K.E., 1996. Looping *P*–*T* paths and high-*T*, low-*P* middle crustal metamorphism: Proterozoic evolution of the southwestern United States. Geology 24, 1119–1122.

Williams, M.L., Jercinovic, M.J., 2000a. Age mapping and dating of monazite on the electron microprobe: Implications for thermo-tectonic analysis of metamorphic rocks. GeoCanada 2000, 731.

Williams, M.L., Jercinovic, M.J., 2000b. Application of electron microprobe age mapping and dating of monazite. Microscopy and Microanalysis 6 (Supplement 2), 406–407.

Williams, M.L., Jercinovic, M.J., Terry, M., 1999a. High resolution "age" mapping, chemical analysis, and chemical dating of monazite using the electron microprobe: a new tool for tectonic analysis. Geology 27, 1023–1026.

Williams, M.L., Karlstrom, K.E., Lanzirotti, A., Read, A.S., Bishop, J.L., Lombardi, C.E., Pedrick, J.N., Wingsted, M.B., 1999b. New Mexico middle crustal cross-sections: 1.65 Ga macroscopic geometry, 1.4 Ga thermal structure and continued problems in understanding crustal evolution. Rocky Mountain Geology 34, 53–66.

Williams, M.L., Jercinovic, M.J., Kopf, C., Hanmer, S., Baldwin, J., Bowring, S., 2000. Microprobe monazite geochronology: an essential tool for regional thermo-tectonic studies of the Western Churchill Province. GeoCanada 2000, 911.

Wingsted, M.B., 1997. Microstructural history of the southern Picuris Range, north-central New Mexico: implications for the nature and timing of tectonism in the southwestern United States. M.S. thesis, University of Massachusetts.

Zhu, X.K., O'Nions, R.K., Belshaw, N.S., Gibb, A.J., 1997. Significance of in-situ SIMS chronometry of zoned monazite from the Lewisian granulites, northwest Scotland. Chemical Geology 135, 35–53.